MOLECULAR AND CELLULAR BIOLOGY, Aug. 2006, p. 6299–6307 Vol. 26, No. 16
0270-7306/06/$08.00+0 doi:10.1128/MCB.00702-06

Bloom Helicase and DNA Topoisomerase IIIα Are Involved in the Dissolution of Sister Chromatids

Masayuki Seki,[1]* Takayuki Nakagawa,[1] Takahiko Seki,[1] Genta Kato,[1] Shusuke Tada,[1] Yuriko Takahashi,[1] Akari Yoshimura,[1] Takayuki Kobayashi,[1] Ayako Aoki,[1] Makoto Otsuki,[1] Felix A. Habermann,[2] Hideyuki Tanabe,[3] Yutaka Ishii,[4,5] and Takemi Enomoto[1,6]

Molecular Cell Biology Laboratory, Graduate School of Pharmaceutical Sciences, Tohoku University, Aoba 6-3, Aramaki, Aoba-ku, Sendai 980-8578, Japan[1]; Ludwig-Maximilians-Universitat, Lehrstuhl fur Tieranatomie II, Veterinarstrasse 13, D-80539 Munchen, Germany[2]; Biosystems Science, School of Advanced Sciences, The Graduate University for Advanced Studies, Shonan Village, Hayama, Kanagawa 240-0193, Japan[3]; Department of Medical Genetics and Radiation Biology, Graduate School of Medicine, Osaka University, Suita, Osaka 565-0871, Japan[4]; Shujitsu University, School of Pharmacy, Nishigawara, Okayama 703-8516, Japan[5]; and Tohoku University 21st Century COE Program "Comprehensive Research and Education Center for Planning of Drug Development and Clinical Evaluation," Sendai, Miyagi 980-8578, Japan[6]

Received 24 April 2006/Returned for modification 26 May 2006/Accepted 2 June 2006

Bloom's syndrome (BS) is an autosomal disorder characterized by predisposition to a wide variety of cancers. The gene product whose mutation leads to BS is the RecQ family helicase BLM, which forms a complex with DNA topoisomerase IIIα (Top3α). However, the physiological relevance of the interaction between BLM and Top3α within the cell remains unclear. We show here that Top3α depletion causes accumulation of cells in G_2 phase, enlargement of nuclei, and chromosome gaps and breaks that occur at the same position in sister chromatids. The transition from metaphase to anaphase is also inhibited. All of these phenomena except cell lethality are suppressed by *BLM* gene disruption. Taken together with the biochemical properties of BLM and Top3α, these data indicate that BLM and Top3α execute the dissolution of sister chromatids.

Eukaryotic *TOP3* was first identified in *Saccharomyces cerevisiae* as a gene that is required to suppress recombination between repeated sequences (28). Deletion of *TOP3* results in a slow-growth phenotype that is suppressed by the disruption of *SGS1*, the gene encoding the sole RecQ helicase in *S. cerevisiae* (5). Further analyses revealed that the function of Sgs1 is closely associated with that of DNA topoisomerase III (Top3) (2, 13, 19, 27). The close relationship between RecQ helicases and Top3 seems to be maintained in higher eukaryotes. Higher eukaryotic cells have two Top3s, Top3α and Top3β (8, 22, 23). Knocking out the *Top3*α gene in mice results in embryonic lethality (17), while knocking out *Top3*β does not affect development but reduces the life span (15). Various Top3 and RecQ helicase molecules have been reported to interact physically, including Top3α and BLM (35), one of the RecQ family helicases in higher eukaryotic cells (3). BLM is a causative gene for Bloom's syndrome (3), which is an autosomal disorder characterized by predisposition to a wide variety of cancers (6). Biochemical analyses have suggested that BLM and Top3α together affect the in vitro resolution of a recombination intermediate containing a double Holliday junction (HJ) via a double-junction dissolution mechanism (34). However, the phenotypes of cells that lack Top3α have not been characterized precisely, since *TOP3*α knockout is lethal. Furthermore, the phenotypes of Top3α-depleted cells before they die have not been examined. Moreover, the physiological relevance of the interaction between BLM and Top3α within the cell remains unclear. Therefore, elucidating higher eukaryotic Top3α function may enhance our understanding of the physiological roles of BLM.

In this study, to assess the function of Top3α and its interactions with BLM, we constructed cells whose expression of Top3α can be switched off by doxycycline hydrochloride (Dox) treatment. To our knowledge, we present the first evidence to support the hypothesis that vertebrate Top3α together with the BLM helicase executes the dissolution of sister chromatids during DNA replication.

MATERIALS AND METHODS

Plasmid construction. Fragments of chicken *TOP3*α and *TOP3*β cDNAs were obtained by PCR from a λ*ZAPII* chicken cDNA library using primers designed from the human *TOP3*α and *TOP3*β gene sequences. The terminal regions of the cDNAs were obtained from chicken testis RNA by 3′ or 5′ rapid amplification of cDNA ends. Genomic DNA fragments of the *TOP3*α and -β genes were amplified by long-range PCR using genomic DNA from DT40 cells. Targeting constructs used to disrupt *TOP3*α were made by replacing the region encoding the active site of Top3α with a neomycin or histidinol selection marker cassette. Targeting constructs for *TOP3*β disruption were made in an analogous manner using a puromycin or blastidin selection marker cassette. Targeting constructs used to disrupt *WRN* and *BLM* have been described previously (12, 29). To construct an expression plasmid carrying mouse *TOP3*α cDNA (22) with the tet-off promoter, a cDNA encoding mouse FLAG-tagged Top3α was inserted into the pUHG10-3 vector.

Gene disruption. DT40 cells (1×10^7) were electroporated with a Gene Pulser (Bio-Rad, Hercules, CA) at 550 V and 25 μF in the presence of 30 μg linearized targeting constructs. Drug-resistant colonies were selected in 96-well plates with medium containing 2 mg/ml neomycin, 1 mg/ml histidinol, 0.5 μg/ml puromycin, or 30 μg/ml blastidin. The disruption of the targeted gene(s) was checked by

* Corresponding author. Mailing address: Molecular Cell Biology Laboratory, Graduate School of Pharmaceutical Sciences, Tohoku University, Aoba 6-3, Aramaki, Aoba-ku, Sendai 980-8578, Japan. Phone: (81) 22-795-6875. Fax: (81) 22-795-6873. E-mail: seki@mail.pharm.tohoku.ac.jp.

TABLE 1. DT40 strains used in this study

Genotype	Disrupted gene(s) (selective marker)[a]	Expression plasmid
Wild type		
BLM$^{-/-}$	*BLM* (His/Bsr)	
WRN$^{-/-}$	*WRN* (His/Bsr)	
*TOP3*α$^{-/-}$	*TOP3*α (Neo/His)	FLAG-m*TOP3*α:Hyg
*TOP3*β$^{-/-}$	*TOP3*β (Puro/Bsr)	
*TOP3*β$^{-/-}$/*TOP3*α$^{-/-}$	*TOP3*β (Puro/Bsr), *TOP3*α (Neo/His)	FLAG-m*TOP3*α:Hyg
*TOP3*α$^{-/-}$/*BLM*$^{-/-}$	*TOP3*α (Neo/His), *BLM* (Puro/Bsr)	FLAG-m*TOP3*α:Hyg
*TOP3*β$^{-/-}$/*BLM*$^{-/-}$	*TOP3*β (Puro/Bsr), *BLM* (Neo/His)	
*TOP3*α$^{-/-}$/*WRN*$^{-/-}$	*TOP3*α (Neo/His), *WRN* (Eco/Bsr)	FLAG-m*TOP3*α:Hyg
RAD51$^{-/-}$	*RAD51* (Neo/Bsr)	Hs*RAD51*:Hyg
MRE11$^{-/-}$	*MRE11* (His/Bsr)	Gd*MRE11*:Hyg

[a] Selective markers: Neo, neomycin; His, histidinol; Bsr, blasticidin; Hyg, hygromycin; Puro, puromycin; Eco, mycophenolic acid.

Southern blotting, genomic PCR, and reverse transcriptase PCR. The genotypes of all of the cell lines used in this study are listed in Table 1.

Western blotting analysis. Cells (1×10^6) were cultured in the presence or absence of Dox, a derivative of tetracycline, harvested, washed with phosphate-buffered saline (PBS), precipitated, and suspended in sodium dodecyl sulfate sample buffer containing 20 mM *N*-ethylmaleimide. Samples were fractionated in a linear 4 to 20% gradient sodium dodecyl sulfate-polyacrylamide gel. Proteins were transferred onto a polyvinylidene difluoride membrane (Millipore) and immunoblotted with anti-*Xenopus laevis* Top3α polyclonal antibody, followed by a horseradish peroxidase-conjugated anti-rabbit immunoglobulin G (IgG) (New England Biolabs) secondary antibody. Bands were visualized using ECL detection reagents (Amersham Pharmacia Biotech).

Growth curve. Cells (2×10^4) were inoculated and cultured at 39.5°C for the specified time periods. Cell samples were counted, and the growth rates were estimated from these data.

Cell cycle analysis. Cells (1×10^6) were washed with PBS and then processed with a Cycle TEST PLUS DNA reagent kit (Becton Dickinson). Cells were filtered through a nylon mesh and analyzed by FACScan (Becton Dickinson). The data obtained were processed by Cell Quest (Becton Dickinson).

Immunocytochemistry. Immunofluorescent staining of whole cells was performed as follows. Cells were collected onto slides with a cytocentrifuge, fixed in 3% paraformaldehyde in PBS for 15 min at room temperature, permeabilized in 0.5% Triton X-100 in PBS for 15 min at room temperature, rinsed three times in 0.5% bovine serum albumin, and incubated for 1 h at 37°C with rabbit anti-MCM4, mouse monoclonal anti-BrdU, and rabbit anti-Ser10-phosphorylated histone H3. Binding of primary antibodies was then detected using fluorescein isothiocyanate (FITC)-conjugated goat or rabbit anti-mouse IgG or Cy3-conjugated goat anti-rabbit IgG. Nuclei were counterstained with 0.2 μg/ml DAPI (4′,6′-diamidino-2-phenylindole).

Detection of chromosome aberrations. Cells were cultured in the presence of 0.1 μg/ml colcemid for 2 h. The cells were harvested and treated with 75 mM KCl for 11 min at room temperature and fixed with methanol/acetic acid (3:1) for 30 min. The cell suspension was dropped onto ice-cold wet glass slides and air dried. The cells were stained with 2% Giemsa solution at pH 6.8 for 25 min and examined by light microscopy.

FISH analysis. Chromosomal aberrations were examined using fluorescent in situ hybridization (FISH) analysis. The macrochromosomes, 1, 2, 3, 4, 5, and Z, and other smaller chromosomes were distinguished by FISH analysis after three-colored painting of chromosomes, as described previously (7). Chromosomes were counterstained with 0.2 μg/ml DAPI.

Detection of early apoptotic cells by flow cytometry. Apoptotic cells were detected using Vybrant apoptosis assay kit no. 3 (Molecular Probes). Cells (1×10^6) were washed with ice-cold PBS and suspended in 100 μl annexin-binding buffer, and 5 μl of FITC-conjugated annexin V and 1 μl of 100 μg/ml PI were added to the cell suspension. After a 15-min incubation at room temperature, 400 μl annexin-binding buffer was added to the cell suspension, and cells were filtered through nylon mesh and analyzed by FACScan. The obtained data were processed with Cell Quest software (Becton Dickinson).

Nucleotide sequence accession numbers. The chicken *TOP3*α and -β cDNA sequences have been deposited in GenBank with accession numbers AB215104 and AB215105, respectively.

RESULTS

***TOP3*α is an essential component of vertebrate cells.** To understand the physiological roles of vertebrate Top3s, we generated *TOP3*α and -β knockout cells using chicken DT40 cells (Fig. 1a and c) (33). The *TOP3*β$^{-/-}$ DT40 cells were constructed by transfecting two *TOP3*β targeting vectors sequentially into wild-type DT40 cells. The *TOP3*α$^{-/-}$ cells were generated by first disrupting one *TOP3*α genomic locus, transfecting the cells with a plasmid expressing the FLAG-tagged mouse *TOP3*α gene from the tet-off promoter, and then disrupting the second *TOP3*α genomic locus. Treatment of these cells with Dox suppresses the expression of the mTop3α protein and results in cells with the *TOP3*α$^{-/-}$ genotype. This circumvents the lethality problem engendered by disruption of both alleles of the *TOP3*α gene. Gene disruption was confirmed by Southern blotting (Fig. 1b and d).

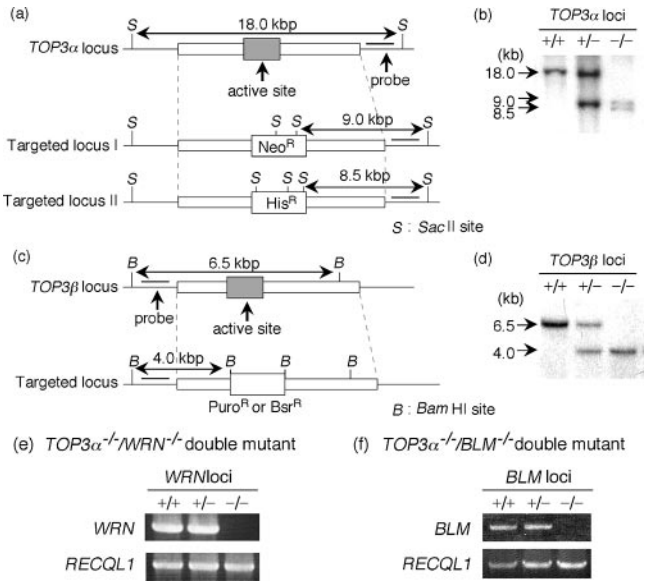

FIG. 1. Generation of *Top3*-disrupted cells. Disruption of the *TOP3*α and *TOP3*β genes. (a) Schematic representation of the *TOP3*α genomic locus before (*TOP3*α locus) and after (targeted locus) the targeted disruption. Probes are indicated by thick lines. The predicted fragments and fragment lengths observed in Southern blot analysis are indicated. (b) Southern blot analysis of wild-type (+/+), heterozygous (+/−), and homozygous (−/−) *TOP3*α-disrupted cells. In *TOP3*α$^{-/-}$ cells, a transgene expressing FLAG-tagged mTop3α was introduced. SacII-digested genomic DNA was hybridized with the probe shown in panel a. (c) Schematic representation of the *TOP3*β genomic locus before (*TOP3*β locus) and after (targeted locus) the targeted disruption. Probes are shown by thick lines, and the predicted fragment sizes are indicated to the left of the Southern blot. (d) Southern blot analysis of wild-type (+/+), heterozygous (+/−), and homozygous (−/−) *TOP3*β-disrupted cells. BamHI-digested genomic DNA was hybridized with the probe shown in panel c. (e and f) Reverse transcriptase PCR analysis of the disruption of *WRN* (e) and *BLM* (f) in the *TOP3*α$^{-/-}$+*FLAG-mTOP3*α background. Wild-type (+/+), heterozygous (+/−), and homozygous (−/−) mutant cells were examined for the expression of *WRN* or *BLM* mRNA. *RECQL1* was also amplified as a control.

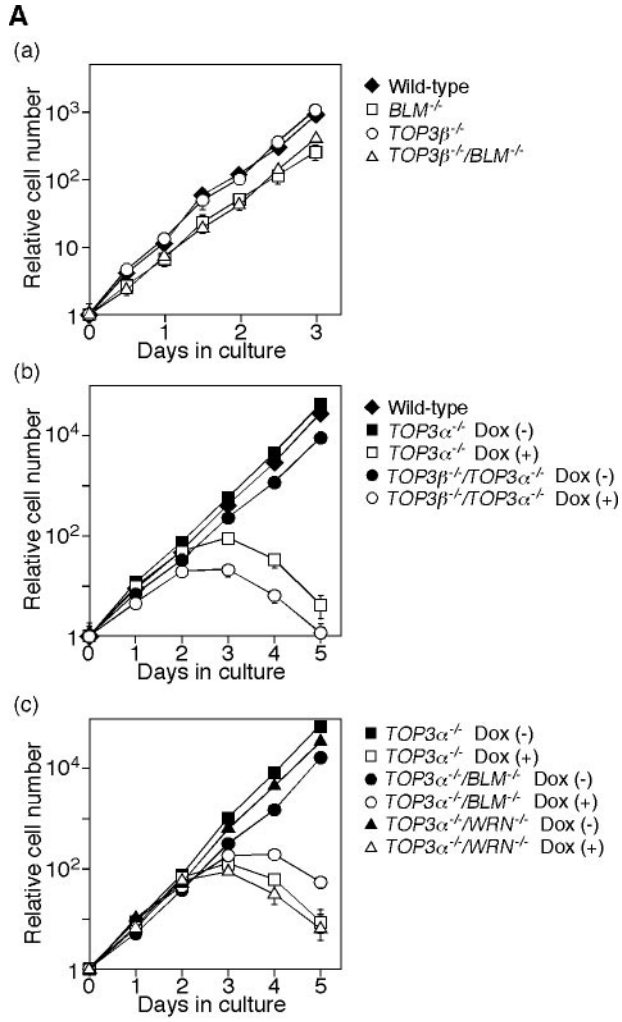

FIG. 2. Growth curves of various *TOP3* mutants. (A) (a) *TOP3*β$^{-/-}$ cells, *BLM*$^{-/-}$ cells, and *TOP3*β$^{-/-}$/*BLM*$^{-/-}$ double mutant cells, (b) *TOP3*α$^{-/-}$ cells and *TOP3*α$^{-/-}$/*TOP3*β$^{-/-}$ double mutant cells in the presence or absence of Dox, and (c) *TOP3*α$^{-/-}$, *TOP3*α$^{-/-}$/*WRN*$^{-/-}$, and *TOP3* α$^{-/-}$/*BLM*$^{-/-}$ cells in the presence or absence of Dox were inoculated at 2×10^4 cells in 3 ml of RPMI 1640 supplemented with 100 μg/ml kanamycin, 10% fetal bovine serum, and 1% chicken serum. The cell densities were measured after the cells were cultured at 39.5°C for the specified time periods. Bars indicate the standard deviations. (B) Disappearance of mTop3α in *TOP3*α$^{-/-}$+*FLAG-mTop3*α cells after Dox treatment. The mTop3α protein was detected by Western blotting using an anti-*X. laevis* Top3α antibody. The expression of α-tubulin served as a loading control.

Figure 2 shows the growth curves of the different DT40 cell lines. The *TOP3*β$^{-/-}$ cells grew at the same rate as DT40 wild-type cells (Fig. 2A, panel a). In the absence of Dox, the *TOP3*α$^{-/-}$ and *TOP3*α$^{-/-}$/*TOP3*β$^{-/-}$ cells grew at the same rate, which was slightly lower than that of wild-type cells. However, both *TOP3*α$^{-/-}$ and *TOP3*α$^{-/-}$/*TOP3*β$^{-/-}$ cells ceased growing within 3 days after Dox addition (Fig. 2A, panel b) The amount of mTop3α in the cells was markedly decreased after Dox treatment (Fig. 2B).

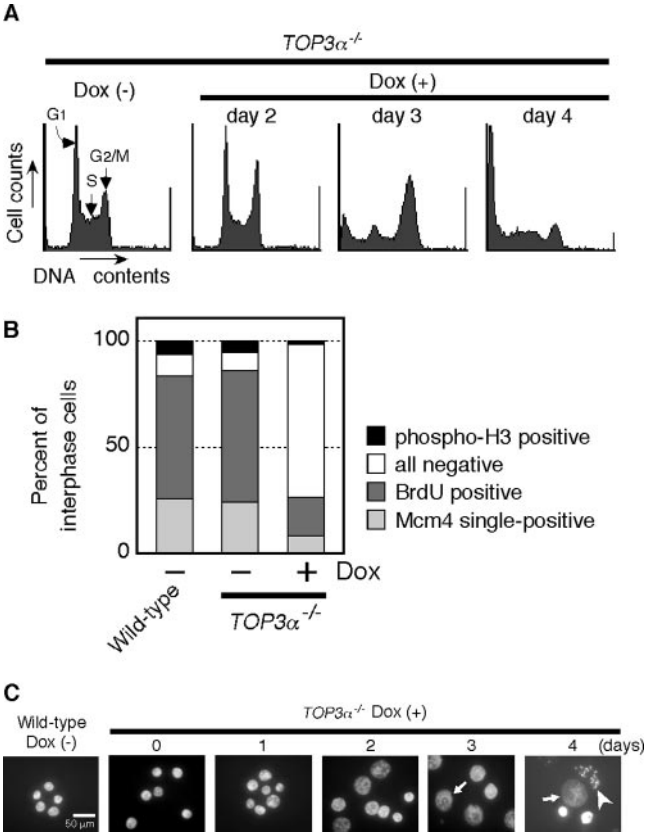

FIG. 3. G_2 arrest of Top3α-depleted cells. (A) Flow cytometric analysis of the effect of Dox treatment on the cell cycle of *TOP3*α$^{-/-}$ cells. *TOP3*α$^{-/-}$ cells (1×10^6) were cultured in the absence or presence of Dox for 2, 3, or 4 days and analyzed using the CycleTEST PLUS DNA reagent kit. (B) Immunostaining analysis of interphase cells. *TOP3*α$^{-/-}$ cells treated with Dox for 3 days were stained with a combination of either rabbit anti-MCM4 and mouse anti-BrdU or mouse anti-BrdU and rabbit anti-Ser10-phosphorylated H3. The binding of the primary antibodies was detected using FITC-conjugated anti-mouse IgG and Cy3-conjugated anti-rabbit IgG. The fractions of cells positive for Mcm4 but not BrdU (Mcm4 single-positive), for BrdU (BrdU positive), and for Ser10-phosphorylated H3 (phospho-H3 positive) were calculated relative to the total number of interphase cells and plotted. The fraction of interphase cells that could not be classified into the above three categories was plotted as "all negative." (C) Enlargement of nuclei in Top3α-depleted cells. *TOP3*α$^{-/-}$ cells were cultured in the absence or presence of Dox for 1, 2, 3, or 4 days and observed by microscopy after being stained with DAPI. Representative morphologies of enlarged nuclei are indicated by arrows (giant nuclei) and arrowheads (disrupted nuclei).

***Top3*α-depleted cells arrest primarily in G_2 phase.** Flow cytometric analysis indicated that the cell cycle distribution of *TOP3*α$^{-/-}$ cells was largely unchanged over 2 days following the addition of Dox (Fig. 3A). However, on the third day, the peak corresponding to G_2/M phase became prominent and cells containing less DNA than G_1 cells appeared. These changes increased markedly by the fourth day. To investigate the point of cell cycle arrest more precisely, the proportion of cells in different

TABLE 2. *BLM* gene disruption suppresses the emergence of unscorable metaphase karyotypes in Top3α-depleted cells

Genotype	No. of days after Dox addition	Total no. of cells observed[a]	No. of unscorable cells	No. of scored cells	No. of aberrant cells[b]	No. of cells with the following chromatid type:			No. of cells with the following chromosome type:	
						Gap	Break	Exchange	Gap	Break
Wild type		200	0	200	16	10	3	0	3	1
BLM$^{-/-}$		200	0	200	19	10	5	0	2	2
*TOP3*α$^{-/-}$		200	0	200	18	9	3	0	2	5
*TOP3*α$^{-/-}$/*BLM*$^{-/-}$		200	0	200	17	5	4	1	6	1
*TOP3*α$^{-/-}$	3	241	41	200	79	16	14	0	34	80
*TOP3*α$^{-/-}$	4	329	129	200	104	16	21	2	28	132
*TOP3*α$^{-/-}$/*BLM*$^{-/-}$	3	201	1	200	54	7	11	1	12	30
*TOP3*α$^{-/-}$/*BLM*$^{-/-}$	4	203	3	200	64	10	11	1	11	43
*TOP3*α$^{-/-}$	3 (2-AP given at 1 h)	277	77	200	109	0	0	3	88	104

[a] Since unscorable metaphase cells were markedly increased in Top3α-depleted cells, we examined from 200 to 329 metaphase cells of various mutants in order to score a total of 200 metaphases per cell line.
[b] Data are presented as the number of aberrations per 200 metaphases.

cell cycle stages was quantified using cell cycle marker-specific antibodies. Thus, cells in G_1 to S phase, S phase, and late G_2 phase were identified by the presence of nuclear staining of MCM4, BrdU, and Ser-10-phosphorylated histone H3, respectively. There was a remarkable increase in the proportion of cells that did not stain with any of these antibodies 3 days after the addition of Dox (Fig. 3B). These data suggest that depletion of Top3α caused a large population of the cells to arrest in G_2 phase before histone H3 was phosphorylated. Moreover, the nuclei of a significant number of the cells were enlarged after the 3-day incubation with Dox and disrupted nuclei were also observed. On the fourth day, there was a marked increase in the number of cells with disrupted nuclei (Fig. 3C).

Appearance of metaphase cells with highly aberrant chromosomes following depletion of Top3α. Although the number of M-phase cells was decreased by the depletion of Top3α, a small but appreciable number of metaphase cells continued to be detected on the third and fourth days after Dox addition. When we examined the chromosomes of these cells, we found a significant increase in chromosome-type gaps and breaks (Table 2 and Fig. 4A, panels b and c). An increase in chromatid-type gaps and breaks was also observed in the Top3α-depleted cells but was much smaller than the increase in chromosome-type aberrations. Top3α deficiency also led to the emergence of metaphase cells with highly aberrant karyotypes which could not be scored (Fig. 4A, panel d, and Table 2). In these cells, the 12 macrochromosomes found in typical metaphase DT40 cells (Fig. 4A, panel a) could not be identified. Chromosome painting revealed the fragmentation of the macrochromosomes in these Top3α-depleted metaphase cells (Fig. 4B). Similar chromosome-type gaps and breaks have been observed in Rad51- or Mre11-depleted cells (25, 36), but almost no "unscorable" metaphase cells were detected in these cells (Table 3). The extent of chromosomal aberrations found in Top3α-depleted cells was much higher than that found in Rad51- or Mre11-depleted cells.

In Top3α-depleted cells, inhibition of the transition from G_2 to M phase and from metaphase to anaphase is released by the protein kinase inhibitor 2-aminopurine. We next examined the transition from metaphase to anaphase in Top3α-depleted cells by scoring anaphase cells that had condensed chromosomes and dephoshorylated histone H3. The Top3α depletion markedly decreased the ratio of cells in anaphase to the total number of mitotic cells, suggesting that the metaphase-to-anaphase transition was inhibited (Fig. 5A). This result is consistent with the dramatic increase in chromosome-type gaps and breaks, which indicates that double-strand breaks are occurring at the same position in sister chromatids. These data suggest a possibility that the decatenation of sister chromatids is defective in Top3α-depleted cells, reflecting an impediment at a very late stage of DNA replication. If the decatenation of sister chromatids is impaired, the decatenation checkpoint should be activated in Top3α-depleted cells. Treatment with 2-aminopurine (2-AP), an inhibitor of protein kinases, has been reported to override G_2 arrest induced by the failure of DNA topoisomerase II (Topo II)-dependent decatenation (1). To assess whether *TOP3*α$^{-/-}$ cells are arrested in G_2 by a 2-AP-sensitive checkpoint mechanism, *TOP3*α$^{-/-}$ cells were treated with 2-AP after a 3-day incubation with Dox. The proportion of cells in M phase increased remarkably within 1 h after the addition of 2-AP and then declined after 3 h (Fig. 5B). In addition, the number of cells containing irregular-shaped, but not enlarged, nuclei increased 3 h after the addition of 2-AP (data not shown). This result further supports the hypothesis that Top3α depletion may result in an ineffective decatenation of sister chromatids. The reduced metaphase-to-anaphase transition of Dox-treated *TOP3*α$^{-/-}$ cells may also be explained by a defect in the decatenation of sister chromatids. The 2-AP treatment decreased the frequency of enlarged nuclei induced by Dox treatment (Fig. 5C), presumably due to entry into M phase, as described above.

Generation of *TOP3*α$^{-/-}$/*BLM*$^{-/-}$, *TOP3*β$^{-/-}$/*BLM*$^{-/-}$, and *TOP3*α$^{-/-}$/*WRN*$^{-/-}$ double mutant cells. To elucidate the functional relevance of Top3s and RecQ helicases, we generated *TOP3*α$^{-/-}$/*BLM*$^{-/-}$, *TOP3*β$^{-/-}$/*BLM*$^{-/-}$, and *TOP3*α$^{-/-}$/*WRN*$^{-/-}$ double mutant cells. *WRN*, which encodes a RecQ family helicase, is the causative gene of Werner syndrome, which is characterized by premature aging (37). Disruption of *BLM* and *WRN* was confirmed by PCR (Fig. 1e and f). While *TOP3*α$^{-/-}$/*BLM*$^{-/-}$ and *TOP3*α$^{-/-}$/*WRN*$^{-/-}$ cells proliferated at a slightly lower rate than *TOP3*α$^{-/-}$ cells in the absence of Dox, the viable cell numbers of all three Top3α-deficient cell lines declined after

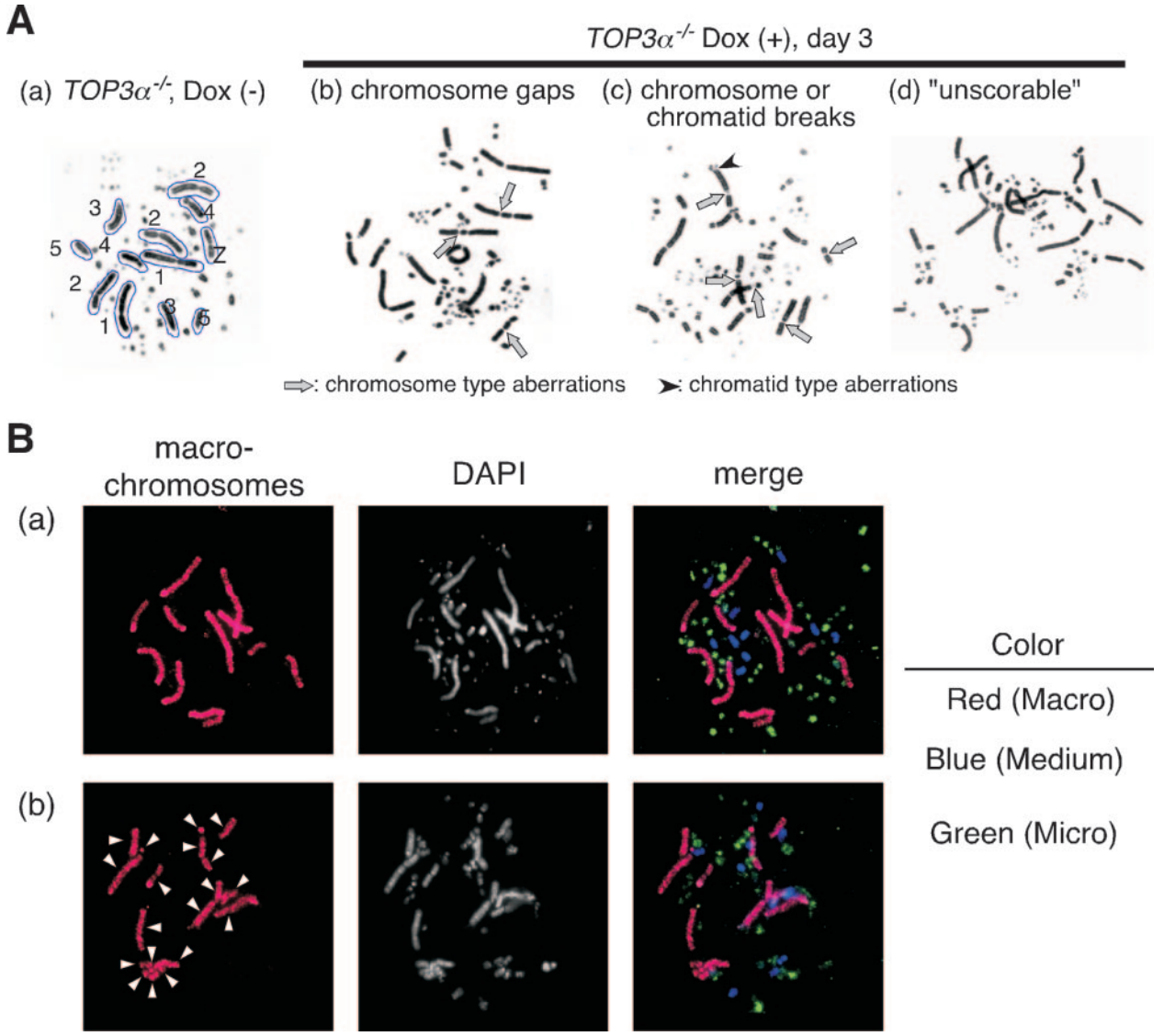

FIG. 4. Chromosomal aberrations in Top3α-depleted cells. (A) The cells were treated with 0.1 μg/ml Colcemid for 2 h before being harvested, and the harvested cells were treated as described in Materials and Methods. (a) The 12 macrochromosomes (1, 3, 4, 5 [two of each], 2 [trisomy], and Z chromosomes) are outlined in a typical image of the metaphase chromosomes in DT40 cells, which was obtained after *TOP3*$^{-/-}$ cells were cultured without Dox. (b and c) Typical chromosomal aberrations observed in Top3α-depleted metaphase cells. Chromosome gaps and breaks are indicated (arrows) along with a chromatid break (arrowhead). (d) A metaphase image in which the 12 macrochromosomes cannot be identified ("unscorable"). (B) Chromosomal aberrations revealed by FISH analysis. The macrochromosomes, 1, 2, 3, 4, 5, and Z, and other smaller chromosomes were distinguished by FISH analysis after three-colored painting of chromosomes, as described previously (7). Red, macrochromosomes; blue, medium-sized chromosomes; green, minichromosomes. (a) *TOP3*α$^{-/-}$ cells cultured in the absence of Dox. Twelve macrochromosomes are indicated by red FISH signals. (b) *TOP3*α$^{-/-}$ cells cultured in the presence of Dox for 3 days. Nineteen red signals derived from macrochromosomes and fragmented macrochromosomes are indicated by arrowheads.

the addition of Dox. However, the cessation of growth of the *TOP3*α$^{-/-}$/*BLM*$^{-/-}$ cells was slightly delayed compared with that of the *TOP3*α$^{-/-}$ or *TOP3*α$^{-/-}$/*WRN*$^{-/-}$ cells (Fig. 2A, panel c). This suggests that unlike WRN, BLM functionally interacts with Top3α. *TOP3*β$^{-/-}$/*BLM*$^{-/-}$ cells grew at the same rate as *BLM*$^{-/-}$ cells (Fig. 2A, panel a). These data indicate that BLM but not WRN functionally interacts with Top3α, while BLM and Top3β do not functionally interact.

Effect of disruption of the *BLM* gene on the phenotypes of *TOP3*α$^{-/-}$-depleted cells. Since our data showed that the disruption of *BLM* did not suppress the lethality of Top3α-depleted cells but did delay the decline of viable cell numbers, we examined in detail the effect of disruption of *BLM* on the phenotypes of Top3α-depleted cells. The mechanism of cell death in *TOP3*α$^{-/-}$, *TOP3*α$^{-/-}$/*BLM*$^{-/-}$, or *TOP3*α$^{-/-}$/*WRN*$^{-/-}$ cells was examined by flow cytometry. In the case of *TOP3*α$^{-/-}$/*BLM*$^{-/-}$ cells, the number of cells that could be stained with an anti-annexin V antibody was markedly increased 4 days after the addition of Dox. In contrast, Dox treatment of *TOP3*α$^{-/-}$ and *TOP3*α$^{-/-}$/*WRN*$^{-/-}$ cells did not lead to a significant increase of annexin V-positive cells (Fig. 6A). These observations indicate that Top3α-depleted *BLM*$^{-/-}$

TABLE 3. No appearance of unscorable metaphase karyotypes in Rad51- and Mre11-depleted cells

Genotype	No. of days after Dox addition	Total no. of cells observed	No. of unscorable cells	No. of scored cells	No. of aberrant cells[a]	No. of cells with the following chromatid type:			No. of cells with the following chromosome type:	
						Gap	Break	Exchange	Gap	Break
RAD51$^{-/-}$		200	0	200	23	8	11	2	6	3
RAD51$^{-/-}$	1	200	0	200	38	9	22	2	15	17
RAD51$^{-/-}$	2	200	0	200	56	9	25	10	24	29
RAD51$^{-/-}$	3	200	0	200	167	21	131	29	68	123
MRE11$^{-/-}$		200	0	200	7	4	0	0	3	0
MRE11$^{-/-}$	5	200	0	200	78	1	9	6	43	43

[a] Data are presented as the number of aberrations per 200 metaphases.

cells died from apoptosis, while Top3α-depleted cells and Top3α-depleted *WRN*$^{-/-}$ cells seem to die by a nonapoptotic pathway.

The occurrence of enlarged nuclei in Dox-treated Top3α-depleted cells was also suppressed by the additional disruption of *BLM* but was not affected by the disruption of *WRN* (Fig. 6B). Both the number of S-phase cells and the number of cells with enlarged nuclei after the addition of Dox were quantified. While *TOP3*α$^{-/-}$ cells showed a decrease in the number of DNA-synthesizing cells and the emergence of enlarged nuclei after Dox treatment for 48 h, *TOP3*α$^{-/-}$/*BLM*$^{-/-}$ cells showed a decrease in S-phase cells only after 78 h and no enlarged nuclei even after 96 h (Fig. 6C). The disruption of *BLM* also suppressed the G_2 arrest (data not shown) and metaphase arrest observed in Top3α-depleted cells (Fig. 5A). Moreover, the disruption of *BLM* in Top3α-depleted cells remarkably reduced the frequency of chromosome-type aberrations and, more importantly, nearly completely suppressed the emergence of "unscorable" metaphase cells which contained chromosomal aberrations too severe to allow us to identify individual chromosomes (Table 2).

DISCUSSION

We show here that Top3α depletion causes accumulation of cells in G_2 phase, enlargement of nuclei, chromosome gaps and breaks that occur at the same position in sister chromatids, and the emergence of "unscorable" metaphase cells. Additionally, the transition from metaphase to anaphase is inhibited. All of these phenotypes were suppressed by *BLM* gene disruption in Top3α-depleted cells.

DNA damage or the failure of sister chromatid dissolution (described below) may cause cells to arrest in G_2 phase, and prolonged arrest in G_2 may subsequently trigger the enlargement of nuclei, similar to that seen with Mre11-depleted cells (36). However, the size of the nuclei is extremely enlarged in Top3α-depleted cells, and thus, it seems likely that packaging of interphase chromatin is somehow affected by the absence of Top3α. This issue must be addressed in future studies.

The result of chromosome aberrations in Top3α-depleted cells is the appearance of chromosome-type gaps and breaks, resulting in a high frequency of "unscorable" metaphase cells. As far as we know, the appearance of "unscorable" metaphase cells is a phenotype unique to Top3α-depleted cells because almost no "unscorable" metaphase cells were detected in Rad51- or Mre11-depleted cells (Table 3). Based on the results obtained in this study, we present two possible mechanisms of BLM and Top3α function, as follows.

Dissolution of sister chromatids. It has been reported that catenanes are formed after DNA replication and are decatenated by Topo II (10, 26). In addition, silencing of human Topo II by small intefering RNA leads to a defect in the dissolution of sister chromatids in human cells (21). Thus, it seems likely that Topo II plays a major role in the dissolution of sister chromatids in eukaryotic cells.

A decade ago, an alternative process for the dissolution of sister chromatids was proposed. An in vitro study using *Escherichia coli* proteins indicated that Topo III efficiently decatenates precatenanes and that when this decatenation does not occur, the daughter molecules (catenanes) remain catenated after DNA replication is completed (9). In addition, it has been proposed that *S. cerevisiae* Sgs1 creates a deleterious topological substrate that Top3 preferentially resolves and that such substrates should be considered precatenanes (5). There is no direct evidence to prove the involvement of Top3 in the dissolution of sister chromatids in the cell. However, our data obtained in this study seem to strongly support the hypothesis that both Top3α and BLM are involved in the dissolution of sister chromatids in vertebrate cells.

If this is the case, the termination intermediates that normally arise when replication forks converge are effectively processed by Top3α and BLM, resulting in the dissolution of sister chromatids. Thus, it is speculated that in the absence of Top3α, the termination intermediates created by BLM are not resolved properly to result in activation of the decatenation checkpoint and/or the formation of double-strand breaks in both sister chromatids, which are observed as chromosome-type aberrations and "unscorable" metaphase cells (Fig. 7A). In the absence of BLM, however, catenanes are formed after DNA replication and can be decatenated by Topo II.

Dissolution of aberrant recombination structures during DNA replication. In *Schizosaccharomyces pombe*, Top3, in conjunction with Rqh1, the sole RecQ helicase in fission yeast, is required for processing or disrupting aberrant recombination structures that arise during S phase (31). Failure of this function leads to the accumulation of aberrant DNA structures, particularly at the ribosomal DNA locus (32), and finally results in unfaithful chromosome segregation (31, 32). Recently, *S. cerevisiae sgs1* mutant cells, which lack the sole RecQ helicase, were found to accumulate damage-induced pseudo double HJs. This suggests that reestablishment of the normal rep-

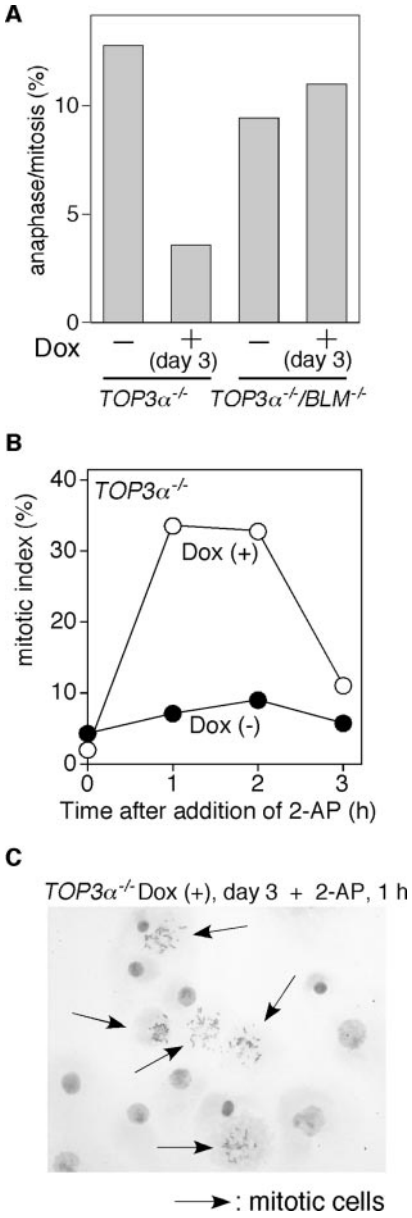

FIG. 5. Reduction of the metaphase transition of Top3α-depleted cells and release from G_2 arrest by 2-AP treatment. (A) Metaphase-to-anaphase transition. Cells in metaphase and anaphase/telophase were identified on the basis of the morphology of the chromosomes and spindles and the existence of phosphorylated histone H3, visualized by staining with DAPI, antitubulin, and anti-phospho-histone H3, respectively. The percentage of telophase/anaphase cells in the total mitotic cell population is shown. (B) Transition of the mitotic index after 2-AP treatment. *TOP3*$\alpha^{-/-}$ cells were cultured in the presence of Dox for 69 h and then exposed to 2-AP for the indicated times. The mitotic index was measured after fixation of the cells. (C) Microscopic image of Top3α-depleted cells after 2-AP treatment. *TOP3*$\alpha^{-/-}$ cells were cultured in the presence of Dox for 69 h and then exposed to 2-AP for 1 h.

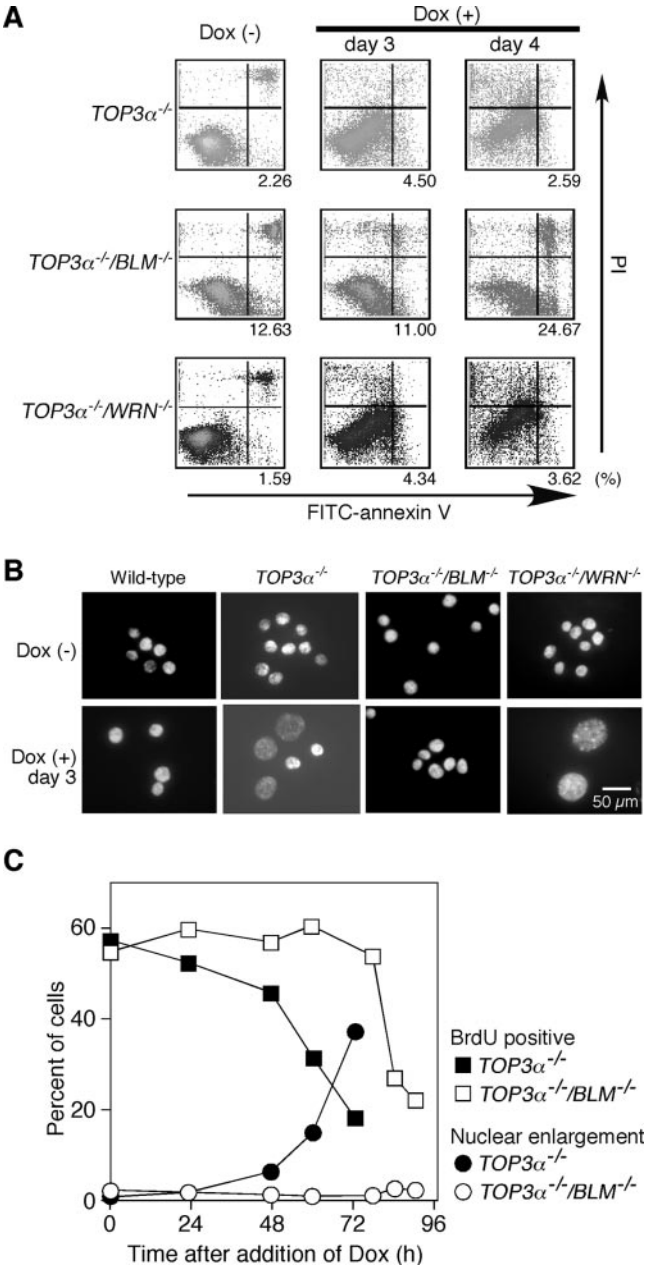

FIG. 6. Induction of apoptosis and suppression of various phenotypes of Top3α-depleted cells by disruption of the *BLM* gene. (A) Detection of apoptotic cells by staining with an anti-annexin V antibody and PI. *TOP3*$\alpha^{-/-}$, *TOP3*$\alpha^{-/-}$/*BLM* $^{-/-}$, and *TOP3*$\alpha^{-/-}$/*WRN* $^{-/-}$ cells were cultured in the absence or presence of Dox for the indicated times and analyzed by flow cytometry after being stained with anti-annexin V antibody and PI by using the Vybrant apoptosis assay kit. The quadrants in the figure indicate living cells (annexin V negative/PI negative, lower left), cells in the early stages of apoptosis (annexin V positive/PI negative, lower right), and dead cells (annexin V positive/PI positive, upper right). Cells in the early stages of apoptosis are indicated as a percentage of the total population. (B) Morphology of *TOP3*$\alpha^{-/-}$ cells with various genetic backgrounds. *TOP3*$\alpha^{-/-}$, *TOP3*$\alpha^{-/-}$/*BLM*$^{-/-}$, and *TOP3*$\alpha^{-/-}$/*WRN*$^{-/-}$ cells were cultured in the absence or presence of Dox for 3 days, after which they were stained with DAPI and their morphology was examined. (C) Effect of disrupting the *BLM* gene in *TOP3*$\alpha^{-/-}$ cells on the appearance of giant nuclei and DNA synthesis. *TOP3*$\alpha^{-/-}$ and *TOP3*$\alpha^{-/-}$/*BLM*$^{-/-}$ cells were cultured in the presence of Dox for the indicated times. Cells that incorporated BrdU or had giant nuclei were counted and expressed as a percentage of the total cell population.

lication fork could be mediated by Sgs1 and Top3, which could collapse the pseudo double HJs back into the four-way sister chromatid junctions that resemble hemicatenanes (Fig. 7B) (18). Interestingly, the pseudo double HJs resemble the termi-

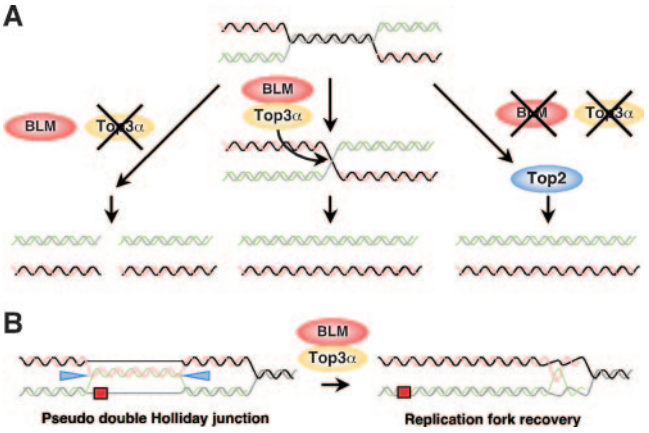

FIG. 7. Model for the dissolution of the structures arisen during DNA replication by Top3α and BLM. (A) Top3α and BLM process the termination intermediates that arise when replication forks converge. (B) Recombination protein mediated template switching type, bypassing DNA lesions at replication forks. Top3α and BLM dissolute the pseudo double Holliday junctions created by recombination proteins to restore normal replication forks. This model is a modified version of Sgs1/Top3 in budding yeast (18).

nation intermediates that arise when replication forks converge (18). Thus, the mechanism that Top3α and BLM resolve sister chromatids is compatible with the above model that Sgs1 and Top3 collapse the pseudo double HJs to restore the replication fork. However, this function of Sgs1 is appreciated only under damage-induced conditions, and the phenomena observed in this study occurred under non-damage-induced conditions. In assessing all of these data, we prefer the former scenario as a model for the mechanism of action of BLM and Top3α in the dissolution of sister chromatids but do not necessarily exclude the second scenario.

Why the lethality of Top3α-depleted cells cannot be suppressed by disruption of *BLM*. Previous studies demonstrated that the lethality of the *top3* mutation in fission yeast was suppressed by deletion of the *rqh1* gene (31). However, disruption of the *BLM* gene did not rescue the lethality of the Top3α depletion in chicken DT40 cells, although several phenotypes observed in the Top3α-depleted cells were suppressed by disruption of *BLM*. This discrepancy may be due to the fact that vertebrate cells carry multiple RecQ helicases (4) which presumably together conduct the functions of the sole RecQ helicases found in unicellular organisms. We have previously suggested that both RECQL1 and RECQL5 may partially replace the function of BLM when it is absent in DT40 cells (30). In addition, human RECQL1 or mouse RECQL5 is required for efficient suppression of sister chromatid exchange even in the presence of their BLM counterparts (11, 16). Given that human RECQL1 interacts with Top3α (14) and human RECQL5 interacts with both Top3α and Top3β (24), it seems likely that vertebrate RECQL1, RECQL5, and BLM perform some overlapping functions. Thus, it is speculated that the partial replacement of BLM function by RECQL1 and/or RECQL5 is responsible for the incomplete suppression by *BLM* deletion of the lethality induced by the loss of *TOP3*α. In spite of the suppression of several phenotypes observed in the Top3α-depleted cells by disruption of *BLM*, *TOP3*$\alpha^{-/-}$/*BLM*$^{-/-}$ cells are still inviable, while *BLM*$^{-/-}$ cells are viable. Thus, it seems likely that Top3α has additional roles separate from those of BLM. Indeed, we previously showed that budding yeast Top3 has roles independent of those of Sgs1 (20). Taken together, the inability to suppress the lethality of Top3α-depleted cells may be due to the combined effect of the presence of multiple RecQs and the defect in additional roles of Top3α independent of those of BLM.

In summary, this is the first detailed report of the phenotype of Top3α-depleted higher eukaryotic cells and has revealed possible roles played by BLM and Top3α in replication. The results obtained in this study help us to understand the function of Top3α and BLM at the molecular level and account for the chromosome instability of Bloom's syndrome cells that arises from defects in BLM function.

ACKNOWLEDGMENTS

We thank O. Imamura, T. Matsumoto, and Y. Furuichi for *WRN* gene targeting vectors.

This work was supported by Grants-in-Aid for Scientific Research on Priority Areas from the Ministry of Education, Science, Sports and Culture of Japan and by Health Sciences Research grants from the Ministry of Health and Welfare of Japan.

REFERENCES

1. **Andreassen, P. R., F. B. Lacroix, and R. L. Margolis.** 1997. Chromosomes with two intact axial cores are induced by G2 checkpoint override: evidence that DNA decatenation is not required to template the chromosome structure. J. Cell Biol. **136:**29–43.
2. **Duno, M., B. Thomsen, O. Westergaard, L. Krejci, and C. Bendixen.** 2000. Genetic analysis of the *Saccharomyces cerevisiae* Sgs1 helicase defines an essential function for the Sgs1-Top3 complex in the absence of *SRS2* or *TOP1*. Mol. Gen. Genet. **264:**89–97.
3. **Ellis, N. A., J. Groden, T. Z. Ye, J. Straughen, D. J. Lennon, S. Ciocci, M. Proytcheva, and J. German.** 1995. The Bloom's syndrome gene product is homologous to RecQ helicases. Cell **83:**655–666.
4. **Enomoto, T.** 2001. Functions of RecQ family helicases: possible involvement of Bloom's and Werner's syndrome gene products in guarding genome integrity during DNA replication. J. Biochem. **129:**501–507.
5. **Gangloff, S., J. P. McDonald, C. Bendixen, L. Arthur, and R. Rothstein.** 1994. The yeast type I topoisomerase Top3 interacts with Sgs1, a DNA helicase homolog: a potential eukaryotic reverse gyrase. Mol. Cell. Biol. **14:**8391–8398.
6. **German, J.** 1993. Bloom syndrome: a Mendelian prototype of somatic mutational disease. Medicine **72:**393–406.
7. **Habermann, F. A., M. Cremer, J. Walter, G. Kreth, J. von Hase, K. Bauer, J. Wienberg, C. Cremer, T. Cremer, and I. Solovei.** 2001. Arrangements of macro- and microchromosomes in chicken cells. Chromosome Res. **9:**569–584.
8. **Hanai, R., P. R. Caron, and J. C. Wang.** 1996. Human *TOP3*: a single-copy gene encoding DNA topoisomerase III. Proc. Natl. Acad. Sci. USA **93:**3653–3657.
9. **Hiasa, H., R. J. DiGate, and K. J. Marians.** 1994. Decatenating activity of *Escherichia coli* DNA gyrase and topoisomerases I and III during *oriC* and pBR322 DNA replication *in vitro*. J. Biol. Chem. **269:**2093–2099.
10. **Holm, C., T. Stearns, and D. Botstein.** 1989. DNA topoisomerase II must act at mitosis to prevent nondisjunction and chromosome breakage. Mol. Cell. Biol. **9:**159–168.
11. **Hu, Y., X. Lu, E. Barnes, M. Yan, H. Lou, and G. Luo.** 2005. Recql5 and Blm RecQ DNA helicases have nonredundant roles in suppressing crossovers. Mol. Cell. Biol. **25:**3431–3442.
12. **Imamura, O., K. Fujita, C. Itoh, S. Takeda, Y. Furuichi, and T. Matsumoto.** 2002. Werner and Bloom helicases are involved in DNA repair in a complementary fashion. Oncogene **21:**954–963.
13. **Ira, G., A. Malkova, G. Liberi, M. Foiani, and J. E. Haber.** 2003. Srs2 and Sgs1-Top3 suppress crossovers during double-strand break repair in yeast. Cell **115:**401–411.
14. **Johnson, F. B., D. B. Lombard, N. F. Neff, M. A. Mastrangelo, W. Dewolf, N. A. Ellis, R. A. Marciniak, Y. Yin, R. Jaenisch, and L. Guarente.** 2000. Association of the Bloom syndrome protein with topoisomerase IIIα in somatic and meiotic cells. Cancer Res. **60:**1162–1167.
15. **Kwan, K. Y., and J. C. Wang.** 2001. Mice lacking DNA topoisomerase IIIβ develop to maturity but show a reduced mean lifespan. Proc. Natl. Acad. Sci. USA **98:**5717–5721.

16. **LeRoy, G., R. Carroll, S. Kyin, M. Seki, and M. D. Cole.** 2005. Identification of RecQL1 as a Holliday junction processing enzyme in human cell lines. Nucleic Acids Res. **33:**251–6257.
17. **Li, W., and J. C. Wang.** 1998. Mammalian DNA topoisomerase IIIα is essential in early embryogenesis. Proc. Natl. Acad. Sci. USA **95:**010–1013.
18. **Liberi, G., G. Maffioletti, C. Lucca, I. Chiolo, A. Baryshnikova, C. Cotta-Ramusino, M. Lopes, A. Pellicioli, J. E. Haber, and M. Foiani.** 2005. Rad51-dependent DNA structures accumulate at damaged replication forks in *sgs1* mutants defective in the yeast ortholog of BLM RecQ helicase. Genes Dev. **19:**39–350.
19. **Mullen, J. R., V. Kaliraman, S. S. Ibrahim, and S. J. Brill.** 2001. Requirement for three novel protein complexes in the absence of the Sgs1 DNA helicase in *Saccharomyces cerevisiae*. Genetics **157:**03–118.
20. **Onodera, R., M. Seki, A. Ui, Y. Satoh, A. Miyajima, F. Onoda, and T. Enomoto.** 2002. Functional and physical interaction between Sgs1 and Top3 and Sgs1-independent function of Top3 in DNA recombination repair. Genes Genet. Syst. **77:**1–21.
21. **Sakaguchi, A., and A. Kikuchi.** 2004. Functional compatibility between isoform α and β of type II DNA topoisomerase. J. Cell Sci. **117:**047–1054.
22. **Seki, T., M. Seki, T. Katada, and T. Enomoto.** 1998. Isolation of a cDNA encoding mouse DNA topoisomerase III which is highly expressed at the mRNA level in the testis. Biochim. Biophys. Acta **1396:**27–131.
23. **Seki, T., M. Seki, R. Onodera, T. Katada, and T. Enomoto.** 1998. Cloning of cDNA encoding a novel mouse DNA topoisomerase III (Topo IIIβ) possessing negatively supercoiled DNA relaxing activity, whose message is highly expressed in the testis. J. Biol. Chem. **273:**28553–28556.
24. **Shimamoto, A., K. Nishikawa, S. Kitao, and Y. Furuichi.** 2000. RecQ5β, a large isomer of RecQ5 DNA helicase, localizes in the nucleoplasm and interacts with topoisomerases 3α and 3β. Nucleic Acids Res. **28:**1647–1655.
25. **Sonoda, E., M. S. Sasaki, J. M. Buerstedde, O. Bezzubova, A. Shinohara, H. Ogawa, M. Takata, Y. Yamaguchi-Iwai, and S. Takeda.** 1998. Rad51-deficient vertebrate cells accumulate chromosomal breaks prior to cell death. EMBO J. **17:**598–608.
26. **Uemura, T., H. Ohkura, Y. Adachi, K. Morino, K. Shiozaki, and M. Yanagida.** 1987. DNA topoisomerase II is required for condensation and separation of mitotic chromosomes in *S. pombe*. Cell **50:**917–925.
27. **Ui, A., Y. Satoh, F. Onoda, A. Miyajima, M. Seki, and T. Enomoto.** 2001. The N-terminal region of Sgs1, which interacts with Top3, is required for complementation of MMS sensitivity and suppression of hyper-recombination in *sgs1* disruptants. Mol. Genet. Genomics **265:**837–850.
28. **Wallis, J. W., G. Chrebet, G. Brodsky, M. Rolfe, and R. Rothstein.** 1989. A hyper-recombination mutation in *S. cerevisiae* identifies a novel eukaryotic topoisomerase. Cell **58:**409–419.
29. **Wang, W., M. Seki, Y. Narita, E. Sonoda, S. Takeda, K. Yamada, T. Masuko, T. Katada, and T. Enomoto.** 2000. Possible association of BLM in decreasing DNA double strand breaks during DNA replication. EMBO J. **19:**3428–3435.
30. **Wang, W., M. Seki, Y. Narita, T. Nakagawa, A. Yoshimura, M. Otsuki, Y. Kawabe, S. Tada, H. Yagi, Y. Ishii, and T. Enomoto.** 2003. Functional relation among RecQ family helicases RecQL1, RecQL5, and BLM in cell growth and sister chromatid exchange formation. Mol. Cell. Biol. **23:**3527–3535.
31. **Win, T. Z., A. Goodwin, I. D. Hickson, C. J. Norbury, and S. W. Wang.** 2004. Requirement for *Schizosaccharomyces pombe* Top3 in the maintenance of chromosome integrity. J. Cell Sci. **117:**4769–4778.
32. **Win, T. Z., H. W. Mankouri, I. D. Hickson, and S. W. Wang.** 2005. A role for the fission yeast Rqh1 helicase in chromosome segregation. J. Cell Sci. **118:**5777–5784.
33. **Winding, P., and M. W. Berchtold.** 2001. The chicken B cell line DT40: a novel tool for gene disruption experiments. J. Immunol. Methods **249:**1–16.
34. **Wu, L., and I. D. Hickson.** 2003. The Bloom's syndrome helicase suppresses crossing over during homologous recombination. Nature **426:**870–874.
35. **Wu, L., S. L. Davies, P. S. North, H. Goulaouic, J. F. Riou, H. Turley, K. C. Gatter, and I. D. Hickson.** 2000. The Bloom's syndrome gene product interacts with topoisomerase III. J. Biol. Chem. **275:**9636–9644.
36. **Yamaguchi-Iwai, Y., E. Sonoda, M. S. Sasaki, C. Morrison, T. Haraguchi, Y. Hiraoka, Y. M. Yamashita, T. Yagi, M. Takata, C. Price, N. Kakazu, and S. Takeda.** 1999. Mre11 is essential for the maintenance of chromosomal DNA in vertebrate cells. EMBO J. **18:**6619–6629.
37. **Yu, C. E., J. Oshima, Y. H. Fu, E. M. Wijsman, F. Hisama, R. Alisch, S. Matthews, J. Nakura, T. Miki, S. Ouais, and G. M. Martin.** 1996. Positional cloning of the Werner's syndrome gene. Science **272:**258–262.